Numerical modelling of three-dimensional fatigue crack closure: mesh refinement

D. Camas, J. Garcia-Manrique, B. Moreno, A. Gonzalez-Herrera

PII: S0142-1123(18)30127-0
DOI: https://doi.org/10.1016/j.ijfatigue.2018.03.035
Reference: JIJF 4636

To appear in: *International Journal of Fatigue*

Received Date: 15 December 2017
Revised Date: 30 March 2018
Accepted Date: 31 March 2018

Please cite this article as: Camas, D., Garcia-Manrique, J., Moreno, B., Gonzalez-Herrera, A., Numerical modelling of three-dimensional fatigue crack closure: mesh refinement, *International Journal of Fatigue* (2018), doi: https://doi.org/10.1016/j.ijfatigue.2018.03.035

Numerical modelling of three-dimensional fatigue crack closure: mesh refinement

D. Camas[1], J. Garcia-Manrique, B. Moreno, A. Gonzalez-Herrera

Department of Civil and Materials Engineering, University of Malaga,
C/ Doctor Ortiz Ramos, s/n, 29071, Malaga, Spain
Phone +34 951952303; Fax +34 951952601
[1]dcp@uma.es

Abstract

Fatigue crack closure has been studied by means of the finite element method for a long time. Most work has been performed considering bi-dimensional models where the numerical methodology has been developed. A great number of bi-dimensional studies analyses different numerical parameters and optimise them.

Three-dimensional models have extended lately. Nevertheless, the methodology employed was taken from the one developed for bi-dimensional cases. The current computational capabilities allow a comprehensive three-dimensional study of the influence of the different modelling parameters in a similar way to those studies carried out with bi-dimensional models.

In particular, one of the key issues is related to the element size, which has a huge influence on crack opening and closure values. In the present work, a CT aluminium specimen has been modelled three-dimensionally and several calculations have been made in order to evaluate the influence of the mesh size around the crack front. The numerical accuracy is analysed in terms of crack closure and opening values. Classical bi-dimensional recommendations are updated. A similar linear relationship has been identified and a minimum mesh recommendation of 60 divisions of the Dugdale's plastic zone size is made.

Keywords: finite element analysis, fatigue crack closure, element size, crack growth.

Nomenclature

a	Crack length
b	Specimen thickness
E	Elastic modulus
H	Hardening modulus
K_{max}	Maximum stress intensity factor
K_{min}	Minimum stress intensity factor
K_{nccl}	Crack closure node contact criterion
K_{ncop}	Crack opening node contact criterion
K_{ttcl}	Crack closure tip tension criterion
K_{ttop}	Crack opening tip tension criterion
$PICC$	Plasticity induced crack closure
R	Load ratio
r_{pD}	Dugdale's Plastic zone size
s_{me}	Minimum element size at the crack tip
W	Specimen characteristic dimension
α	Constraint factor
δ	Inverse of η
ε_{yy}	*y-strain*
η	Number of divisions of the plastic zone size
σ_y	Yield stress
σ_{yy}	*y*-stress

1. INTRODUCTION

Since the early 70s, finite element models have been intensively used to study the Plasticity Induced Crack Closure (PICC) phenomenon. Although other crack closure mechanisms have been identified [1–3], PICC is usually considered as the fundamental phenomenon that promotes crack closure. According to this theory [4,5], crack growth is largely influenced by the effect of the plastic wake, which is the yielded material developed during previous fatigue load cycles. This wake causes a premature contact of the crack flanks even when a tensile load is applied far from the crack front, delaying the crack growth rate.

Modelling the whole process of crack growth under fatigue loading conditions represents a great complexity. There is a huge number of load cycles implied and high plastic strain concentrated in a small volume of several orders of a smaller magnitude than the size of the analysed specimen, with steep stress gradients. The computational cost when analysing this kind of problems is a significant challenge, in particular when three-dimensional models are considered.

In the literature, a large number of previous studies, which analyse the influence of different numerical parameters on the opening or closure results, can easily be found. Some attempts to optimise the mesh size [6,7], the number of loading cycles between node releases [8] (or crack growths), the simulated plastic wake required to stabilise results [9] and the variable considered to quantify PICC have previously been developed. Nevertheless, due to the computational cost of the problem, most of them are bi-dimensional analyses, considering plane stress or plane strain conditions. In these previous works, some relevant conclusions were found and have been used as a starting point for this study.

In the numerical simulation, one of the most critical issues is the choice of the mesh size near the crack front and in particular, the minimum element size close to the crack front. Smaller elements allow obtaining stress and strain fields more accurately near the crack front. In addition, it makes the crack growth simulation approach closer rates to real crack propagation ones, as it reduces crack growth at each node release. Nevertheless, the use of smaller elements leads to an increase in the computational cost because of two main reasons: the increase in the number of elements of the model and in the number of cycles needed to reach the desired final crack length.

Newman [10] was the first one who examined the mesh refinement problem. He considered a two-dimensional centre-cracked panel under mode I cyclic loading conditions with elastic-plastic material behaviour. The crack growth and the crack closure were analysed under plane stress conditions. In this

work, he showed how the size of the elements close to the crack tip influences the obtained crack closure and opening values. McClung and Sehitoglu [11] also dealt with it, considering a steel with a bilinear kinematic hardening model (H/E=0.007). They employed two different mesh sizes and carried out calculations under different load levels. The mesh size was parameterised with the plastic zone size. Analysing the opening stresses, he recommended dividing the plastic zone size into 20 triangular constant elements or 10 quadrilateral linear elements. This recommendation of 10 linear elements has been considered a universal rule by many subsequent studies. Besides, they noted the important role of reversed plasticity in modelling the crack closure phenomenon. According to Solanki et al. [12], 3-4 linear elements within the reversed plastic zone are necessary, while Roychowdhury and Dodds [13] suggested 2-3 linear elements.

The influence of the element size and the rate of crack growth on the opening loads were analysed by Antunes *et al.* [14]. Considering kinematic and isotropic hardening models, he found that the opening values follow different kinds of behaviour with element size. When decreasing the minimum element size, the number of load cycles or stress loops in the node at the crack tip increases. This can affect the obtained results. In order to study the influence of the element size near the crack tip independently of the number of applied load cycles, he considered a constant crack growth length releasing several nodes at a time depending on the element size, showing the influence on the results when considering a kinematic hardening model.

In a later bi-dimensional analysis considering a C(T) specimen and different linear isotropic hardening models, Gonzalez-Herrera and Zapatero [15] suggested more restrictive mesh sizes than those recommended by McClung. Increasing mesh refinement beyond 10 elements in the forward plastic zone he observed erratic behaviour of the opening and closure results. He considered up to 140 linear elements within Dugdale's plastic zone size in both plane strain and stress conditions, and found nearly stable closure values. However, a linear extrapolation method was proposed in order to obtain the opening and closure values to an ideal zero mesh size.

Parks et al. [16] considered instead a pure kinematic hardening model. They proposed an optimum mesh size determined in terms of the theoretical reversed plastic zone size comparing plane stress numerical results with experimental ones. This optimum element size was in the order of 0.77-0.91 times the reversed plastic size, which means that between one or two elements were needed in the reversed plastic zone size.

There are other more recent studies considering bi-dimensional states that analyse the mesh refinement influence as those developed by Jiang *et al.* [17] and Cochran *et al.*[6]. In the first one, because of the huge computational effort that is necessary to grow the crack long enough to stabilise the opening loads for a highly refined mesh, they recommended an exponential extrapolation of the opening loads with crack length. They found that convergence strongly depends on the material model. In the second one, considering a boundary-layer model, Cochran et al. analysed issues like the numerical crack growth rate and cyclic material response as they correlate to mesh refinement effects on opening loads. Finally, it should be remarked that Antunes *et al.*[7], apart from the influence of the element size close to the crack front, developed an analysis of the size of the most refined region near the crack front considering that this area has a huge influence on computational cost.

In the last years, as computational power has been developed, some three-dimensional studies have appeared [18–23]. In these studies, the developed methodology and the result analysis were proposed for the first time, obtaining crack closure values at plane stress, plane strain and its evolution along the thickness in the three-dimensional case. All these papers considered an elastic-perfectly plastic modelling material and employed the contact node as crack closure criterion. The contact between the crack flanks was simulated considering springs and changing their spring stiffness coefficient depending on the position of the nodes.

The shape of the crack front has a great influence on the stress and strain fields of 3D cracked bodies [24]. The yielded area at the surface of the specimen increases when the radius of curvature decreases. On the contrary, the yielded area in the mid plane only depends on the load applied and the specimen thickness. These behaviours will affect to the stable crack shape.

It is well known, that the crack front in through cracks presents some kind of curvature when the crack grows under fatigue loading conditions. Some efforts have been made in order to explain and characterise the crack front curvature [25–27]. Many adaptative remeshing techniques have been proposed to evaluate crack shape evolution and its influence on fatigue life [28]. However, the crack front is usually considered straight in 3D analysis [29,30]. This simplification allows to be focused on the influence of numerical parameters.

Alizadeh et al. [31] compared two and three-dimensional analyses of fatigue crack closure. They found a good agreement between the three-dimensional finite element crack opening results at the surface and the

bi-dimensional plane stress ones, while the agreement between the results in the mid-thickness and the plane strain ones only occurred for large thicknesses.

A remarkable recent work is the one published by Vor et al. [32]. In this study a 3D model is developed to simulate PICC under constant ΔK configurations with a constant stress ratio R=0.1. The effect of the plastic wake length and the size of through thickness cracks in CT specimens of a stainless steel alloy is considered.

Nevertheless, the methodology usually employed in these previous 3D analyses has been taken from those developed for bi-dimensional states. This way, the element size is usually related to McClung's recommendation.

Therefore, the aim of this work is to analyse, the influence of the mesh size on the accuracy of parameters related with PICC, when considering a three-dimensional model. The numerical precision is analysed in terms of crack closure and opening values along the specimen thickness.

This paper consists of in the following sections. First, the FE analysis methodology used is briefly described. It is based on references and completed with the experience of the present authors. In the next section, the influence of element size on the results is presented. Results are presented in terms of crack opening and closure values. Finally, main recommendations are stated in the conclusions.

2. FEA MODELLING METHODOLOGY

In this section, the general parameters affecting the model are presented. Issues like geometry, meshing and element size, material behaviour, loading cycles and crack growth scheme, contact simulation, plastic wake and opening and closure definition considered in this study are presented.

In this study, a CT specimen geometry (W = 50mm, a = 20mm) has been three-dimensionally modelled, with the material displaying an elastic-plastic behaviour. The commercial FE software ANSYS has been employed for this purpose. Fig. 1 shows a scheme with main dimensions, where a is crack length and b specimen thickness. For this study, a 3mm specimen thickness has been considered. In combination with the load applied (Kmax = 25 MPam½), this thickness represents an intermediate behaviour according to previous studies [33] with a limited computational cost.

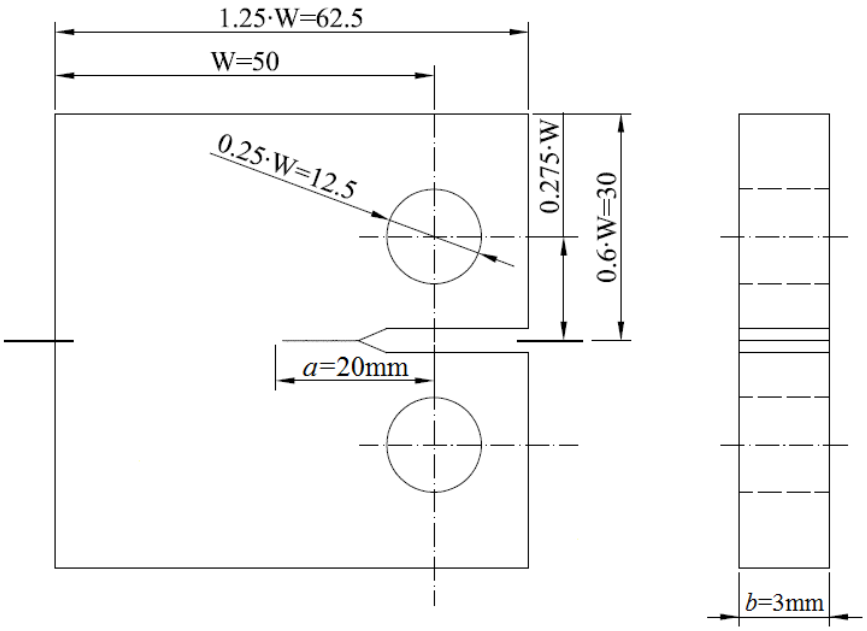

Figure 1. CT specimen dimensions in mm.

2.1. Meshing and element size

The most critical region is the area close to the crack front, where there are huge gradients in the stress and strain fields. Therefore, in order to capture this effect properly, the size of the elements around the crack tip must be sufficiently small. However, in order to reduce the computational cost, to make a huge transition from this zone to the most remote ones is necessary. For this reason, the specimen has been divided in two different areas. In the first one, a homogeneous and uniform structured mesh with hexahedral elements is made around the crack tip. In the second one, an unstructured mesh is considered. These tetrahedral elements are used where material behaviour is elastic during the whole loading process and because they allow the size transition. An advantage from the point of view of the computational cost is the symmetry of the problem. For this reason, just a quarter of the specimen is modelled. Fig. 2 shows the three-dimensional mesh used. The homogeneous region around the crack front and the transition one can clearly be distinguished. It can be seen that a straight crack front has been employed in this study.

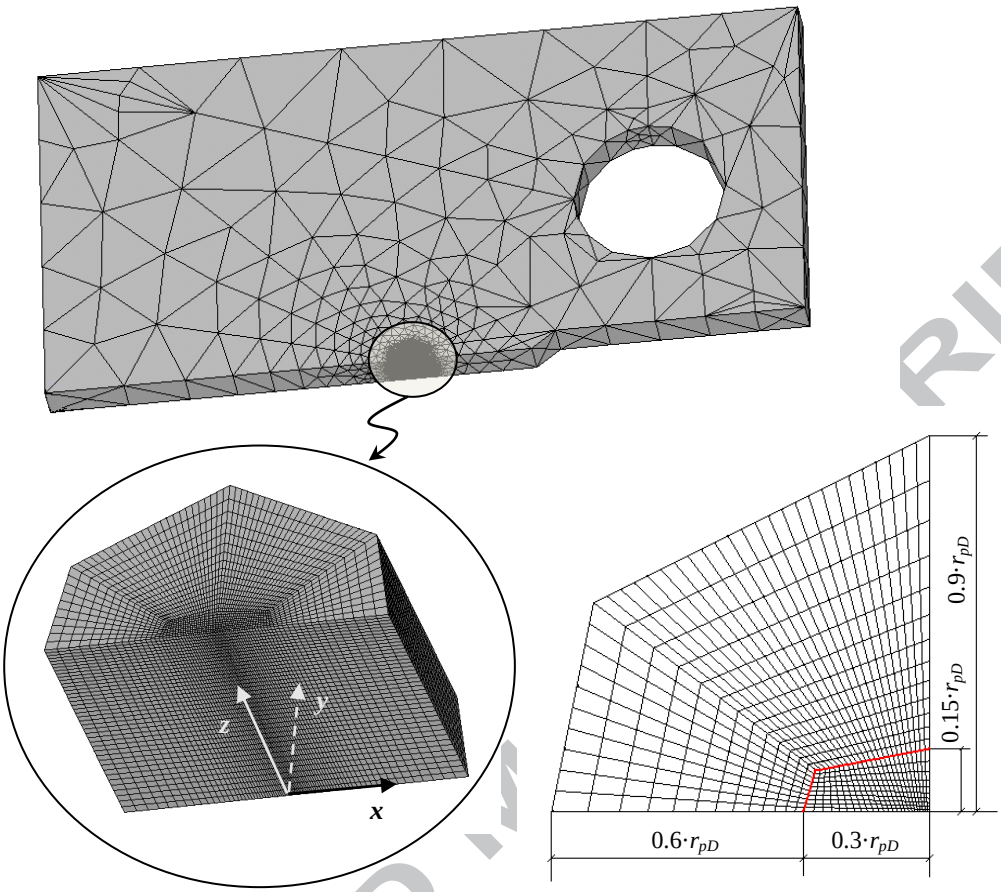

Figure 2. 3D finite element model

In the literature, there is a general agreement on the use of a regular mesh with linear or quadratic square (2D) or hexahedral (3D) elements. However, Gonzalez-Herrera and Zapatero [9] employed a mesh size transition reducing the mesh size with the crack growth. The idea is to get a stress and strain field as continuous as possible reducing the number of load cycles to reach the final crack length and consequently, the computational cost. They showed that if the mesh transition is lower than a 15% reduction of the element sizes, the obtained results do not suffer any significant variation. In the present study, this transition rate has been taken into consideration as an upper limit, allowing only transitions with lower rates than 8% far from the crack front and 4% near the final crack front.

In this study, the minimum element size along the propagation axis (x) is given in terms of the plastic zone size. A dimensionless term defined as

$$\eta = r_{pD} / s_{me} \qquad \text{(eq. 1)}$$

where r_{pD} is the plastic zone size according to Dugdale's equation (eq. 2) and s_{me} is the size of the element at the crack tip (minimum element size). This parameter represents the number of divisions in which the plastic zone would be meshed if a regular lattice of elements equal to the smallest one had been used. A normalised element size δ, defined as the inverse of η is also employed.

$$r_{pD} = \frac{\pi}{8\alpha}\left(\frac{K_I}{\sigma_y}\right)^2 \quad \text{(eq. 2)}$$

Table 1 shows the different values of η considered in this work and their corresponding minimum element sizes, number of elements and nodes of the whole model and in the region near the crack front (in brackets). It can be seen that the element sizes range from 43.5 to 11.2μm.

η	Minimum element size (μm)	Number of elements	Number of nodes
30	48.3	31,336 (14,440)	18,620 (16,195)
50	29.0	42,582 (21,120)	28,557 (23,370)
70	20.7	61,277 (37,120)	45,628 (40,303)
90	16.1	76,353 (47,520)	57,177 (51,250)
110	13.2	105,254 (54,640)	85,026 (58,712)
130	11.2	165,902 (72,160)	143,902 (77,080)

Table 1. Minimum element sizes, number of elements and nodes.

In Dugdale's expression (eq. 2), α is a constraint factor equal to 1 for plane stress and 3 for plane strain. As a 3D model is considered in this work, α has been taken equal to 1 in order to be higher than any yielded zone size along the thickness. According to the load applied in this work (K_{max}=25MPa·m$^{1/2}$), the Dugdale plastic zone size in plane stress is 1.45mm. Previous 3D numerical simulations [24,33] provided a plastic zone size ranging from $0.15 \cdot r_{pD}$ (at the exterior) to a maximum value of $0.6 \cdot r_{pD}$. The yielded area at the surface is really similar to the yielded area in the mid-plane when the crack front is considered straight and its evolution along the thickness is in the same order. The plastic zone size extension is dependent on the specimen thickness and presents different distribution along the thickness. Consequently, considering a constant constraint factor seems appropriate.

As shown in previous studies [24,33,34], in the vicinity of the surface of the specimen, there is a transition area in the plastic zone. Close to the mid plane, where plane strain conditions are dominant, the plastic zone is homogeneous. In order to capture the strain and stress fields properly, the length along the thickness of the element next to the surface is half the length of the element next to the mid plane of the specimen. Outside this region, the number of through-thickness divisions was reduced to speed up the simulations. Fig. 3 shows the meshed employed along the thickness.

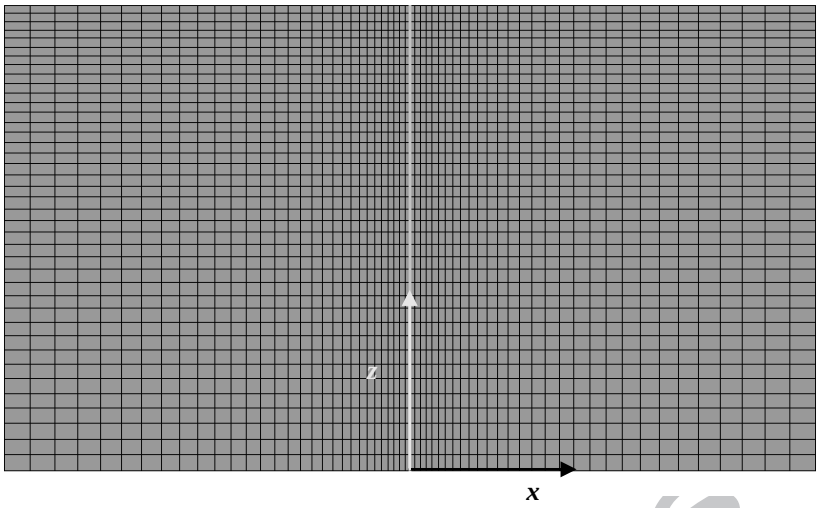

Figure 3. Mesh along the thickness

An eight node element with a linear base function has been used to mesh the specimen where structured mesh was necessary. At each node, there are three degrees of freedom corresponding to the displacements in the *x*, *y* and *z* directions. The tetrahedral elements are obtained degenerating the element, condensing faces to lines and have been used to make the transition easy.

2.2. Material behaviour modelling

The modelled material has been an Al-2024-T351 aluminium alloy that shows weak hardening (E=73.5GPa, σ_y=425MPa, K'=685MPa, n'=0.073, being K' and n' the parameter and the exponent in the Ramberg-Osgood yielding model). In this work, the cyclic stress-strain curve is considered in the numerical model. In this way, the hardening behaviour of the material that is obtained with a huge number of loading cycles is obtained in the model just applying a single load. This strategy allows huge saving on computational cost. The Al-2024-T351 has an average grain size of approximately 138, 67 and 43μm in rolling, transverse and thickness directions respectively [35].

In a previous work [36], this material was numerically modelled in different ways considering bi-dimensional models. This study was carried out considering both isotropic and kinematic hardening models using bi and three-linear diagrams to define the stress-strain curve. Nevertheless, no differences were found in the results when a weak work hardening rule is considered, as in this case. Only noticeable differences were obtained for hardening ratios H/E above 0.03, where the H is the hardening modulus and E the elastic modulus.

When the material has these *H/E* ratios, such as some steel alloys, to analyse the hardening rule and the crack growth scheme deeply is of major importance. However, the convergence of the results is independent of the specific hardening rule employed for the material considered in this study, where *H/E*=0.007. Therefore, a three-linear stress-strain curve with an isotropic hardening law has been used in the present study in order to model the material behaviour.

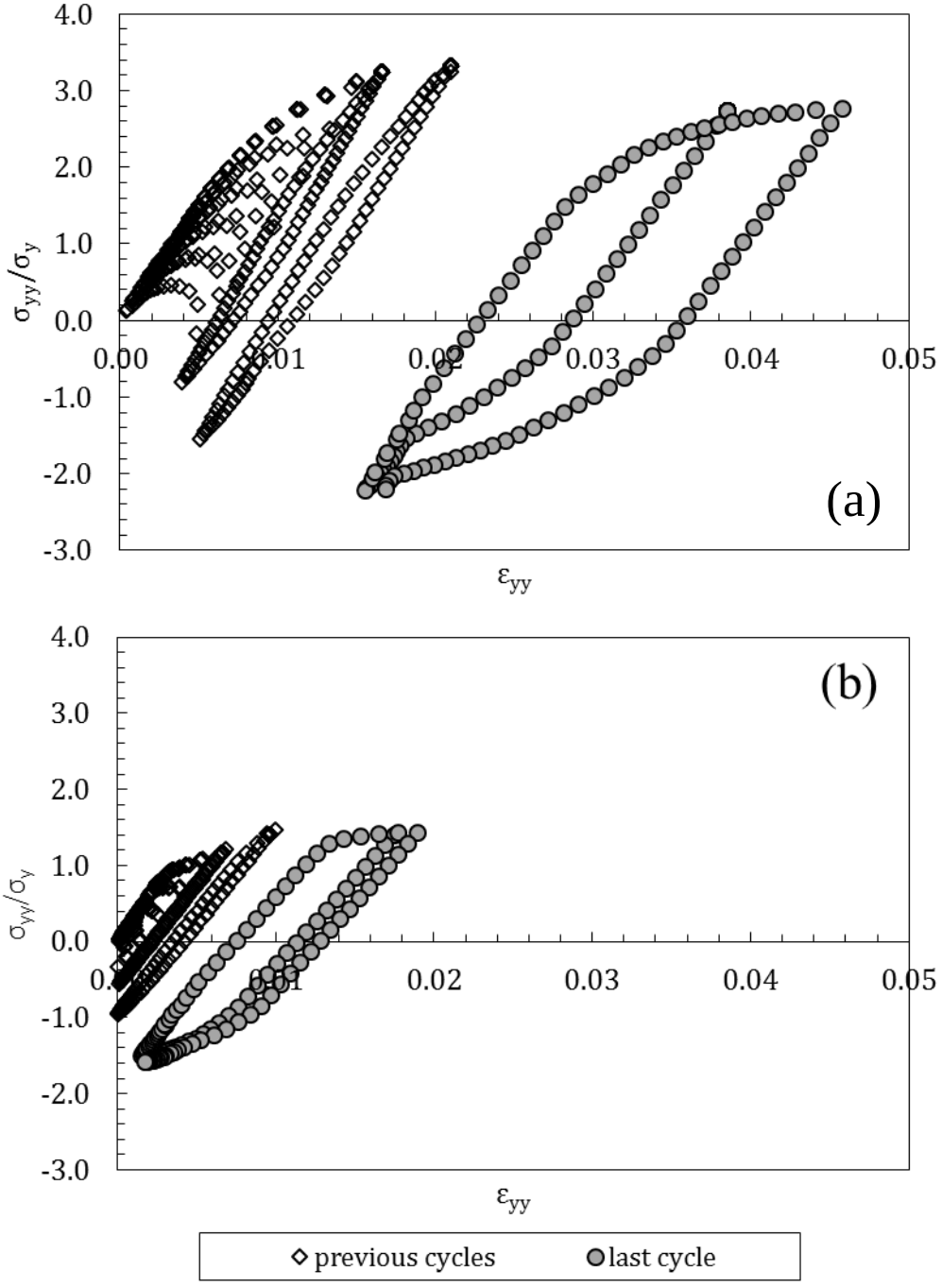

Figure 4. Stress-strain curve for a node in the crack front (a) in the mid-plane and (b) at the surface (K_{max}=25MPa·m$^{1/2}$, R=0.1, η=70) .

Fig. 4 presents the stress-strain curve σ_{yy}-ε_{yy} registered at two different nodes placed at the final crack front during crack propagation. One at the surface and the other one in the mid-plane. The stresses were normalised by the yield stress. At the beginning of crack propagation, the considered nodes are approximately 600μm ahead of the crack front. Although this initial distance, both nodes reaches σ_{yy} slightly higher than the yield stress. From the first cycles, a compressive stress state can be observed in the node at the surface, while the node in the mid-plane needs some cycles to reach that state.

As the crack propagates the distance of both nodes to the crack front reduces and the stress levels increase yielding more plastic deformation, especially in the node located in the mid-plane. The compressive stresses at minimum load also increase and start to develop a reversed plastic deformation. It can be observed that at the final loading cycle the y-stress level in the mid-plane is bigger than at the surface. The σ_{yy} in the mid-plane is 3 times higher than the yield stress at the surface, while at the surface, it is just approximately 1.5 times higher. The compressive stresses in the mid-plane are higher too, although in this case, the difference between both nodes is smaller. It can be clearly seen that there is strain ratchetting in the material behaviour, which is more pronounced in the mid-plane than at the surface.

The results of this figure are obtained considering a R=0.1 and η=70. The mesh refinement implies an increase of the stress and strain values because the Gauss points of the elements are closer to the crack front. The different physical and numerical parameters on stress-strain curves has been broadly studied in the literature [6,11,37].

2.3. Load cycles, crack growth scheme and plastic wake length

Fatigue analysis implies crack growth. In this work, constant amplitude loading conditions with crack growth are considered. A constant maximum load is applied during the crack growth simulation. As the crack growth that must be developed to stabilise results is small, as is shown below, ΔK can be considered as constant during the development of the plastic wake. However, it is important to note that K_{max} considered at each case shown on the results corresponds to the final crack length (a=20mm).

Load is numerically applied at the nodes located in the upper half of the specimen pin hole. The only limitation is that no plasticity has to be introduced during the loading process. If so, the number of nodes has to be increased.

The crack growth scheme is a main issue in this kind of analysis. Each change in loading and boundary conditions means solving a non-linear problem, making it impossible to consider all the cycles involved

in a real fatigue problem using the finite element method, due to the computational cost required. Reducing the mesh size or increasing the number of load cycles between crack propagations up to a more realistic level, has a huge computational cost. A balance between mesh size, plastic wake length developed and the number of applied cycles must be found.

In this work, crack growth is carried out changing the boundary conditions. A node is released at each load cycle in order to obtain a strain field as continuous as possible. The most appropriate moment to release the nodes during the load cycle is unclear. The most accepted criterion is to release nodes at maximum load [11,15,38–40]. However, several authors have pointed out [11,12] that the influence of the load at which the crack growth occurs can be discarded. Anyway, the maximum load has a great physical sense and there are lesser possibilities of numerical instabilities. Therefore, it is the criterion that has been followed in the present study.

So the crack growth is modelled by means of a limited number of cycles, changing the boundary condition from one cycle to the next to simulate the crack advance. This implies an artificial process that must be carefully designed to avoid computational errors.

As a reference for the present work, experiments provide a fatigue crack growth rate (da/dN) ranging from 0.1 to 0.5μm/cycle [41], depending on R and for K_{max}=25MPa·m$^{1/2}$. The minimum element size at the crack tip ranges from 11.2 to 43.5μm. Consequently, this approximately implies from 20 to 430 real cycles per numerical cycle.

With regards to the number of load cycles between node releases, literature has usually performed one or two. However, in three-dimensional analyses usually only one load cycle is applied because of the numerical cost [13,22,30,42]. Some exceptions have recently appeared which analyse the influence of the number of load cycles on the opening and closure stresses considering three-dimensional models. Considering an elastic perfectly plastic material model of a titanium alloy, de Matos and Nowell [43] did not establish the exact number of load cycles between node releases to stabilise the opening stress values for a three-dimensional analysis. However, they concluded that for more than eight load cycles, the influence of the crack growth scheme is very little. Vor et al. [32] considered a stainless steel with strong hardening and rachetting, which is very sensitive to the number of loading cycles. Considering a crack growth of 0.1mm and four releases and comparing the maximum and minimum stresses and strains along

the crack front, they concluded that an optimum was found at 15 cycles between node releases. However, this question still remains.

This work focuses on the influence of element size on the crack opening and closure results. Therefore, the main issue is to keep the rest of numerical parameters that can affect to the results as constants. As said before, crack growth is carried out releasing the next set of nodes at each load cycle, when maximum load is reached. After releasing the nodes, an additional step with constant maximum load is applied in order to stabilise the stress and strain fields to the new boundary conditions. In order to achieve an easier convergence during the first steps of crack growth, the first loading cycles are applied increasing their values gradually without allowing crack growth, until the maximum load has been achieved.

Simulations are carried out considering R=0.1, 0.3 and 0.7. The obtained results in a previous bi-dimensional study [15], provides the starting point for this three-dimensional analysis. The maximum load applied corresponds to a stress intensity factor K=25MPa·m$^{1/2}$. The relationship between the load applied and the stress intensity factor K is determined by equation 3 [44].

$$K = \frac{P}{b\cdot\sqrt{W}}\cdot\left(\frac{2+\frac{a}{W}}{\left(1-\frac{a}{W}\right)^{\frac{3}{2}}}\cdot\left(0.886+4.64\cdot\left(\frac{a}{W}\right)-13.32\cdot\left(\frac{a}{W}\right)^{2}+14.72\cdot\left(\frac{a}{W}\right)^{3}-5.6\cdot\left(\frac{a}{W}\right)^{4}\right)\right) \quad \text{(eq. 3)}$$

The minimum length of the plastic wake that is necessary to simulate is a critical parameter because it influences the obtained results strongly. In the literature, two different main ways of analysing the minimum crack length can be found. The first one [14,16,37] consists of analysing the opening/closure values when increasing the crack length until a stabilised value has been obtained. However, for this option, a regular lattice mesh is necessary, which is not the case in the present study. In the other one [9,30], the final crack length is equal for all the different plastic wake lengths analysed and the difference is that the initial crack front is placed at different distances.

With this approach, the advantages are highlighted as follows: the final results are always obtained in the same place, so no meshing differences affect the results; less data need to be stored, because only data from the last cycle are saved. It yields a more efficient mesh, which reduces the computational cost strongly but maintains the same accuracy. The main disadvantage is that several simulations are needed while with the other method, just one provides the required data.

In this work, the second approach has been followed. From a previous bi-dimensional work which analysed the plastic wake length influence on plane strain and stress conditions [9], a plastic wake length of 0.4 times Dugdale's plastic zone size has been considered before the results was obtained.

2.4. Contact simulation

The contact simulation is a critical issue when crack closure phenomenon is numerically analysed. Without contact between the crack flanks, to develop the plastic wake is not possible. Therefore, no regions near the crack front would be under compression.

Contact problems are highly non-linear and require significant resources to solve them. Generally, the contact areas are not known before running the simulation. They depend on the applied loads, the material behaviour, boundary conditions and other factors. In the literature, contact has been usually achieved employing springs, truss elements or removing or imposing crack surface nodal constraints [12,38,45].

In this work, contact elements have been employed. These contact elements overlay the region of the solid in which the contact with the target surface is expected. This target surface represents the other flank of the crack. It is considered rigid and is discretised by just one quadrilateral element. This target allows the free tangential displacements, so no friction has been considered between the target and the contact elements.

The Augmented Lagrangian method [46] is used as contact algorithm. This method allows updating the contact stiffness at each load, substep or iteration. This stiffness can be based on different references as the average of the stresses of all the contact elements or on the stress of individual elements. In the simulations developed for this work, the stiffness has been updated at each substep based on the mean stresses from the previous substep of individual elements.

2.5. Opening and closure definition

In this work, in order to determine the crack opening and closure values, two different criteria widely used in the literature [8,43] have been employed. The first one is based on the displacements of the first node behind the crack front. The second one is based on the stresses at the crack front.

The one based on displacements defines the opening when the first node behind the crack front loses contact with the target surface. In other words, it gets a positive *y*-displacement. This criterion is denoted as node contact criterion and is represented with subscript *nc*. The other criterion, based on stresses,

defines the opening when the stress at the node located at the crack front turns from compression into tension. This criterion is denoted as tip tension and is represented with subscript *tt*. Besides, it is important to note that crack opening is denoted with subscript *op* and closure as *cl*. Thus, K_{ncop} and K_{ttop} represent the opening values determined by the node contact and the tip tension criteria respectively, while K_{nccl} and K_{ttcl} represent the closure ones.

The last cycle, which are loading and unloading, in which the data are collected to determine the opening and closure results, is divided in 80 substeps. The interval between load substeps is constant because the opening and closure values has a broad range as depend on the considered criterion and the position along the thickness. Interpolation between known data is considered in order to reduce the introduced error as much as possible due to the fact that information is only available at discrete moments. Increasing the number of substeps in the last cycle increases computational cost, in particular storage requirements. Again, a balance between accuracy and computational cost must be considered.

3. RESULTS

3.1. Bi-dimensional results

The study of the influence of the minimum element size on 2D fatigue crack closure values was widely studied in [15]. A dependence of the tip tension and node contact crack opening values obtained as a function of the minimum element size are summarised in Fig. 5. It can be seen that for the lower element sizes, the opening stress increases gradually until it reaches η values in the order of 20-30 divisions of the plastic zone. In this area, the result seems stable, fitting into McClung's recommendation. Nevertheless, if η is increased, the curve starts to change its trend. Consequently, the opening stress value decreases significantly. The influence of an appropriate reversed plastic zone mesh was considered to be causing this change.

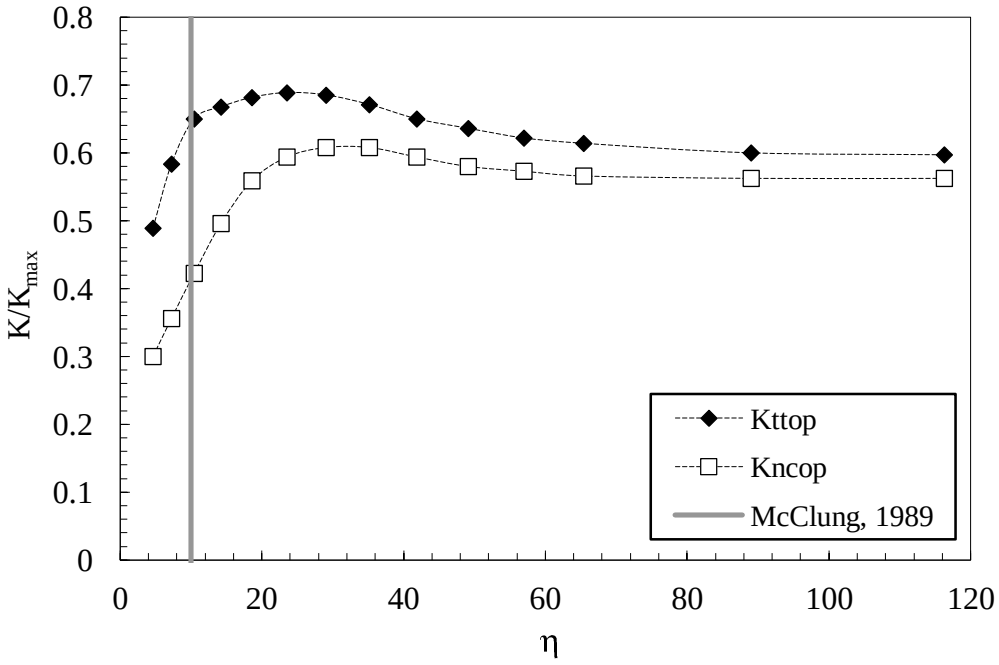

Figure 5. Crack opening values for R=0.3 in terms of η, 2D plane stress. K_{max}=25MPa·m$^{1/2}$.

A new method was suggested to obtain the crack closure and opening values. It can be summarised as the use of at least three different FE models, with different minimum element sizes. The minimum size was recommended to be δ<0.03 for linear elements. From these results, the closure or opening values were obtained by means of a linear extrapolation in terms of δ (see Fig. 6).

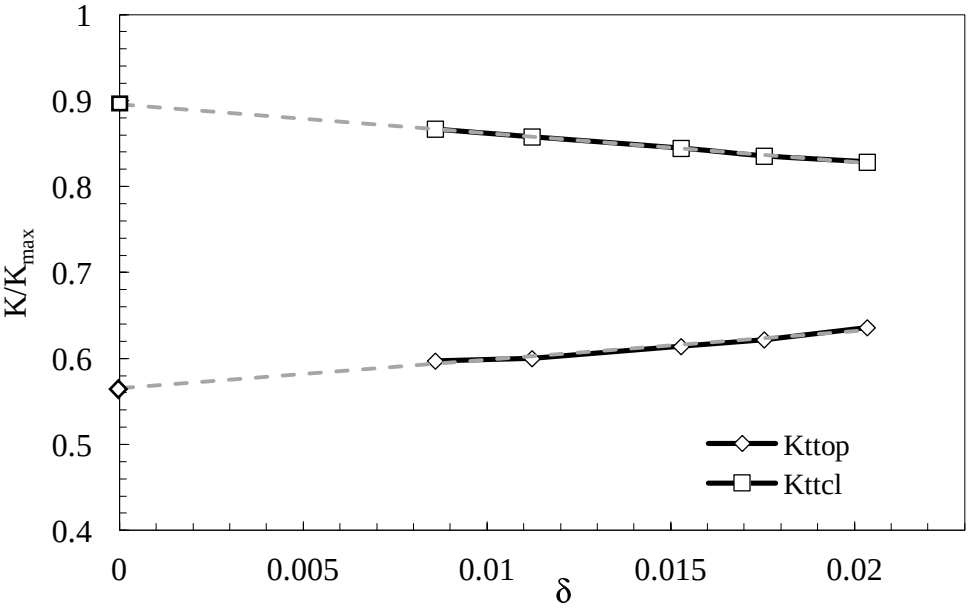

Figure 6. Tip tension opening and closure values for R=0.3 in terms of δ, 2D plane stress.

K_{max}=25MPa·m$^{1/2}$.

It can be seen, that by employing this procedure, the tip tension crack opening value is equal to 0.565, while the crack closure value is 0.895. It can also be interpreted that using a minimum element size 90 times smaller than the Dugdale's plastic zone size, the difference with the ideal zero size element scenario stands below 2%.

3.2. Three-dimensional results

This methodology is also applied considering three-dimensional models. Nevertheless, some key differences must be taken into account. Basically, they are related to the fact that several values are obtained along the crack front. In Fig. 7, the obtained results along the thickness for R=0.1 and 0.3, considering η=90, are shown. The horizontal axis of the figure is the position along the thickness in mm, where the minimum value represents the mid-plane and 1.5 represents the specimen surface. Due to the symmetry, only half of the specimen thickness is represented.

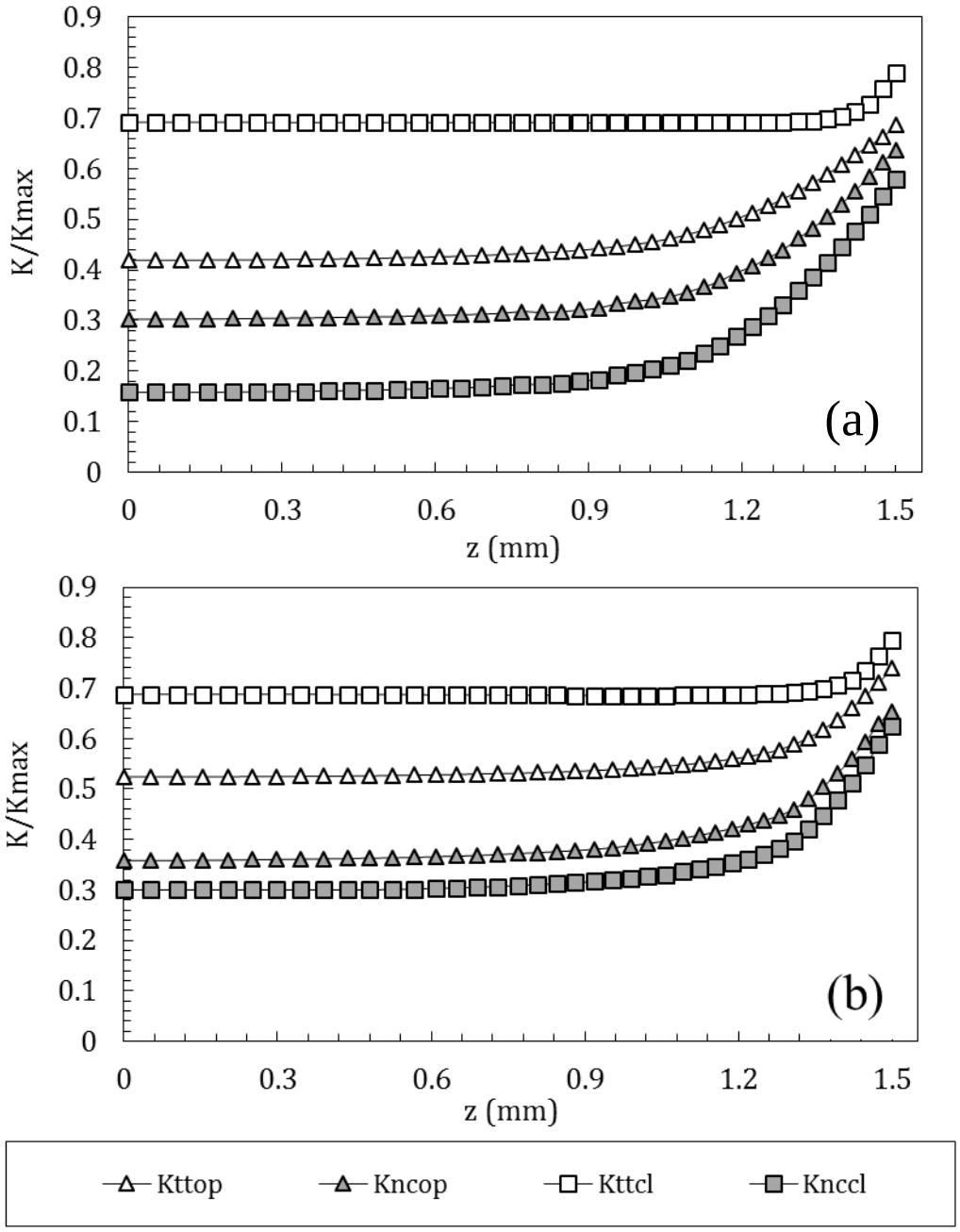

Figure 7. Opening and closure values along the thickness. K_{max}=25MPa·m$^{1/2}$, b=3mm, η=90 and R=0.1 (a), R=0.3 (b).

At first sight, it can be seen that the effect of the crack closure is more prominent close to the surface of the specimen, as expected. There is transition zone near the surface where crack closure values are greater than the constant value achieved in the interior of the specimen. The same tendency is observed for both criteria. The difference is the size of these transition zones and the obtained values. In this work, the length of the transition zone is defined as the distance from the surface until the position along the

thickness where there is a variation of 1% respect $K_{max,}$ higher than the value in the mid-plane. Table 2 shows these results.

	Transition zone length (mm)			
	Kttcl	***Kttop***	***Knccl***	***Kncop***
***R*=0.1**	0.12	0.80	0.83	0.80
***R*=0.3**	0.14	0.64	0.70	0.81

Table 2. Transition zone lengths. K_{max}=25MPa·m$^{1/2}$, b=3mm, η=90.

It can be seen that there is a huge influence of the criterion considered to determine the crack opening or closure value. These values range from 0.12 to 0.83. The tip tension closure values are similar for both stress ratios and completely different with respect the rest of them. The values for R=0.1 are pretty similar for the other criteria, while there are slight differences when considering a R=0.3.

The crack opening and closure values at the surface range from 0.79 to 0.58. In this case, the values are similar when comparing the ones obtained for each criteria for both stress ratios. However, inside the specimen, for R=0.1, the values range from 0.16 to 0.69, while for R=0.3, they range from 0.3 to 0.69. The source of these differences can be the fact that the crack remains open at the minimum load in the interior of the specimen when considering the displacements at R=0.3. Approximately, a third of the specimen thickness is open, while the other two thirds of the surface are closed. Although stresses are in compression and consequently the crack is considered as closed, the no contact between the crack flanks is affecting to the transition zone of the opening values. It can be seen that for R=0.1, the contact of the flanks in the interior of the specimen takes place at a value just below 0.2.

The evolution of the results with the element sizes in terms of δ has to be plotted to analyse the influence of the minimum element size. For clarity, in Fig. 8 the crack opening values obtained with both criteria, tip tension and node contact, are represented for nine different planes along the thickness. As before, the minimum value represents the mid-plane and 1.5 refers to the surface. The case represented in this figure corresponds to a load ratio R=0.1. In this figure, six different element sizes have been represented , which are 30 to 130 times smaller than Dugdale's plastic zone size.

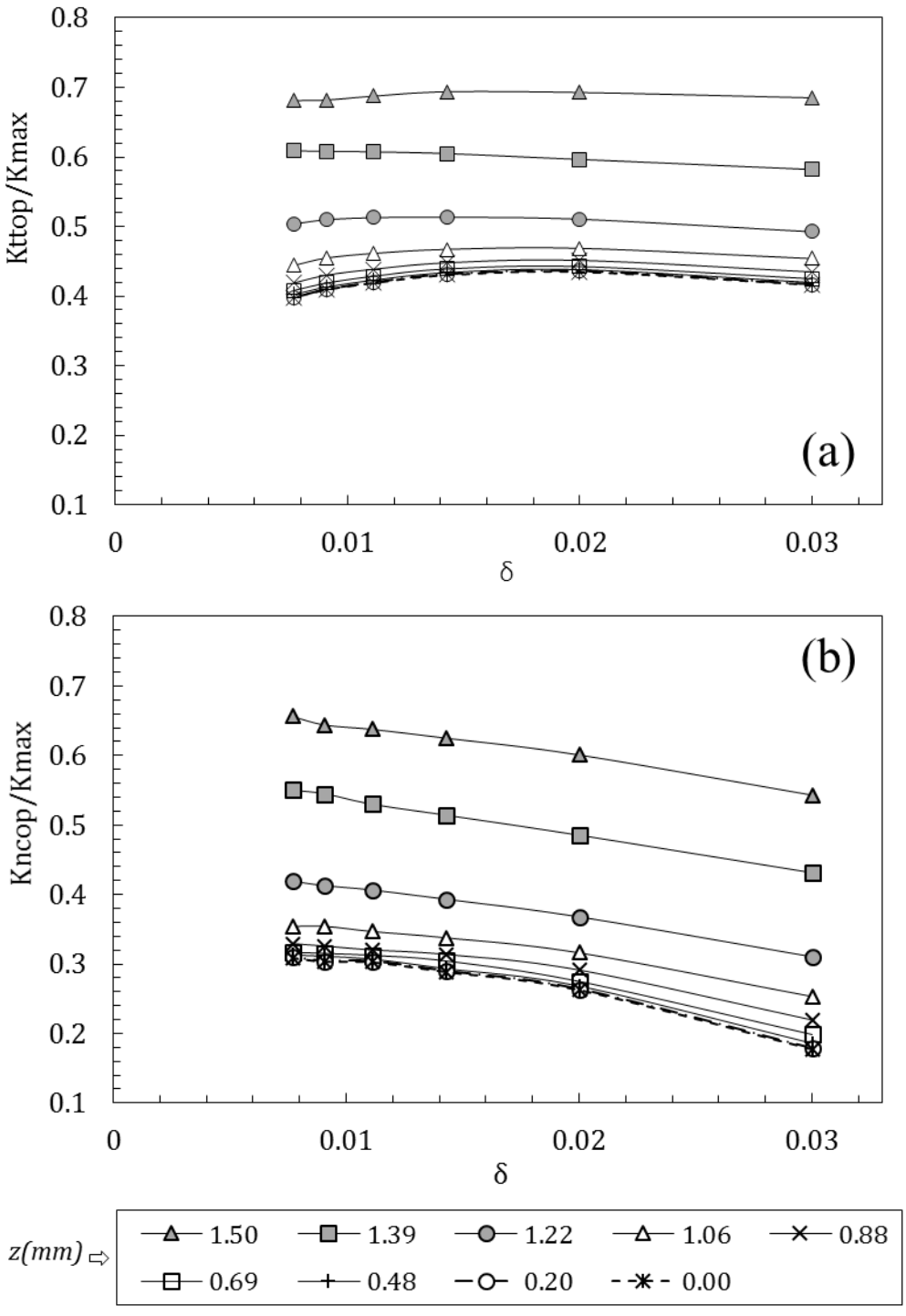

Figure 8. K_{ttop} (a) and K_{ncop} (b) evolution with δ for some planes along the thickness. K_{max}=25MPa·m$^{1/2}$ and R=0.1.

It can be observed that the evolution is very stable. In the tip tension criteria, the obtained results are almost constant for the planes closest to the surface, while the results fall in relationship with the δ decrease near the mid-plane. On the other hand, the same behaviour can be seen for all the planes along the thickness when analysing the node contact opening values. A linear relationship is found between the

opening values and the minimum element size in terms of δ. The opening values slightly increase when δ decreases.

The curves were linearly extrapolated to obtain the results with an ideally minimum element size equal to zero. A result for δ=0 was obtained as can be observed in Fig. 9. For clarity, only data from five different planes along the thickness have been plotted in these figures.

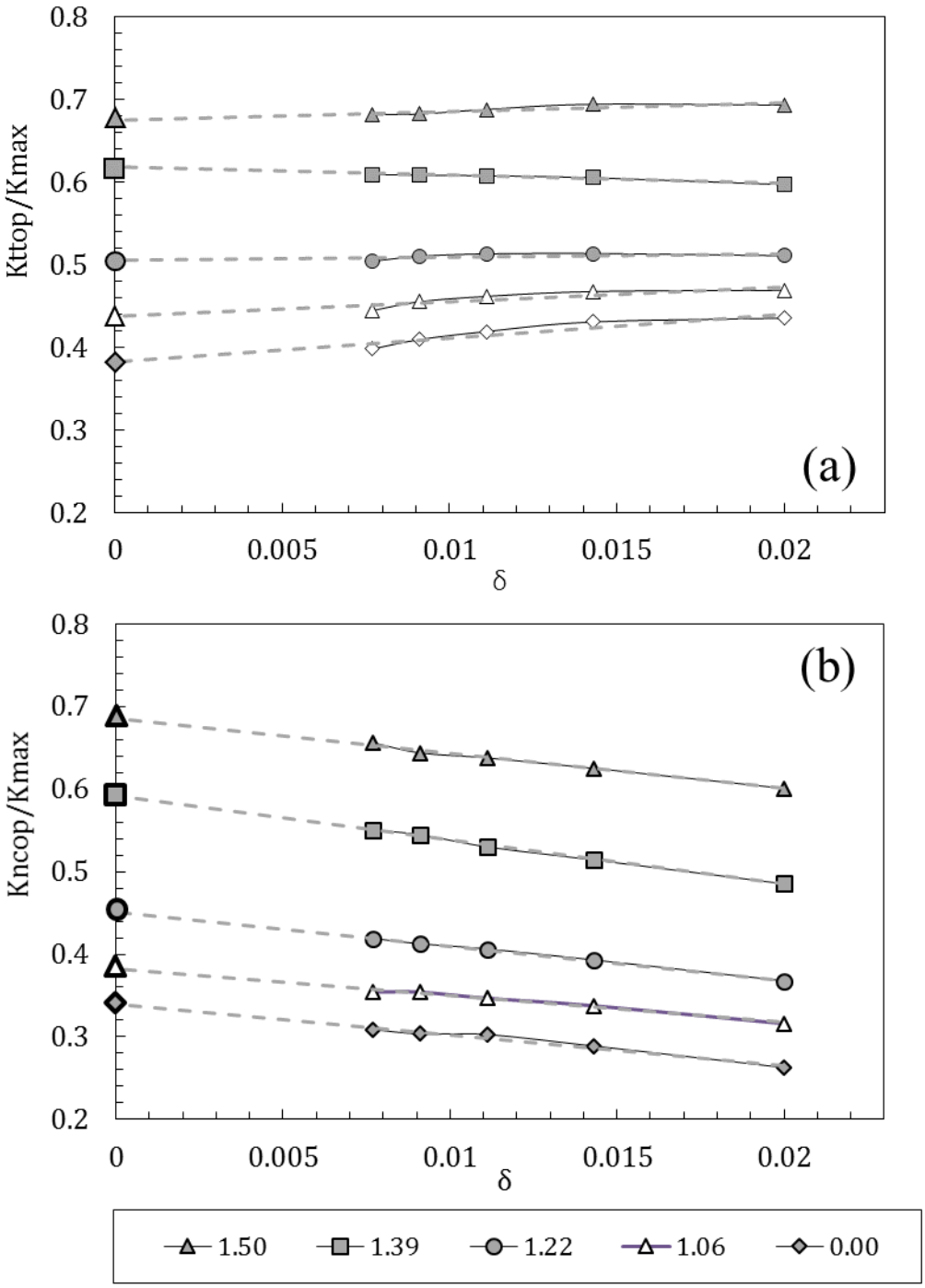

Figure 9. K_{ttop} (a) and K_{ncop} (b) linear extrapolation. K_{max}=25MPa·m$^{1/2}$ and R=0.1.

These figures represent the value that should be obtained with a null element size, which correspond to the representation of a continuous medium (with an infinite number of divisions). Therefore, it seems reasonable to take these values as the most accurate ones for crack opening or closure.

The suitability of employing this linear extrapolation can be discussed when considering the tip tension opening values, especially in the interior of the specimen. Maybe, it would be more appropriate to consider a second order polynomic interpolation or a linear one, just considering smaller element sizes in the order of δ=0.015. In both cases the results would be similar. The opening values in the interior of the specimen decreasing and bringing them closer to the node contact results. However, for this analysis, the linear interpolation is followed considering the bi-dimensional recommendations.

In Fig. 10, the ideal opening values obtained all along the thickness for the R=0.1 case are represented carrying out a linear extrapolation. It can be observed that the differences obtained between both opening criteria are much smaller considering the ideal results than the data obtained considering a minimum element size equal to η=90.

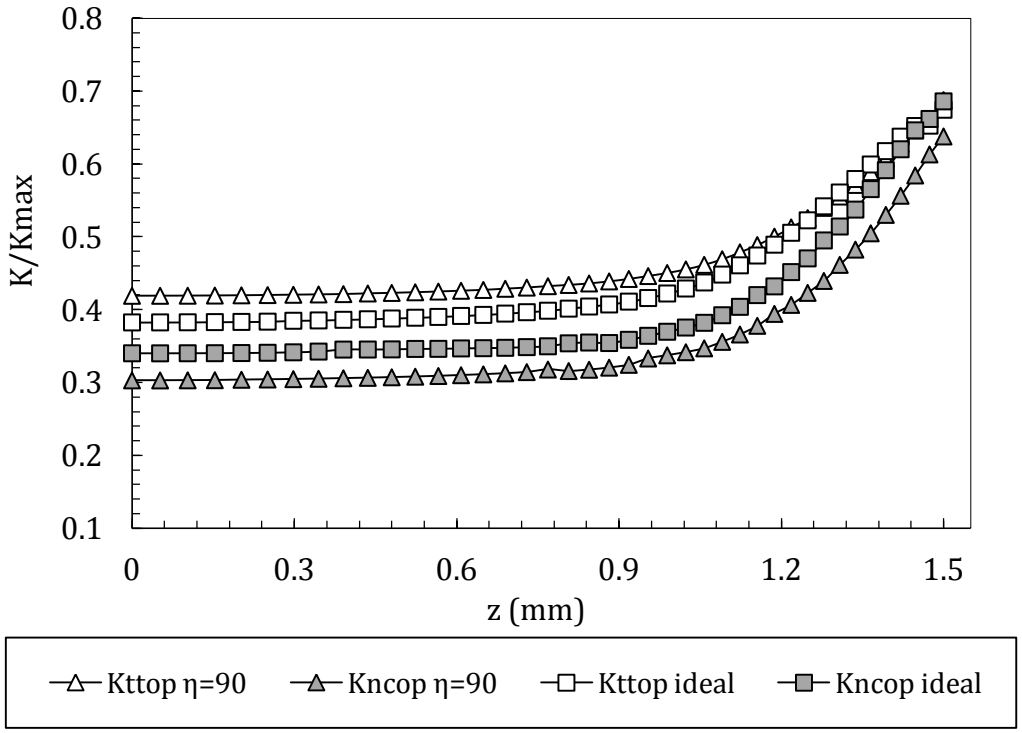

Figure 10. Opening results considering ideal element size or η=90. K_{max}=25MPa·m$^{1/2}$ and R=0.1.

Although this extrapolation process leads to better results, like in the bidimensional case [15], the computational cost of the three-dimensional problem makes it difficult to adopt this methodology. In this

sense, it seems of more interest to evaluate the deviation with the minimum element size and consequently, choose the mesh size depending on the accuracy required. If this deviation is in the order of other uncertainties that affect the analysed problem, the increase of computational cost to avoid them would not be justified.

In Fig. 11, this deviation for opening and closure results is evaluated for two different mesh sizes, being η=90 and 110. It is considered as the difference between the obtained results for the element sizes and the linear extrapolation ones, normalised by the stress intensity factor corresponding to the maximum load applied. In Fig. 11(a), the opening results are shown. It can be observed that the deviation for the criterion based on stresses is almost null close to the surface. It increases as we move into the interior, without exceeding a difference greater than 5% in any case. Obviously, the smaller the minimum element size, the lower the difference with the one considered as the most accurate value. It can be seen that the deviation remains practically around 4% all along the thickness when analysing the results based on the node contact criterion. However, they are slightly greater near the surface.

Focusing on crack closure results, as seen in Figure 11(b), the node contact results are of the same order as before, while the results based on the stress fields are much greater and in the order of 10%. These values are justified, because the tip tension crack closure values have a strong dependence on the minimum element size. They show strong linear behaviour similar to the node contact opening behaviour shown in Figure 9(b), but even more pronounced.

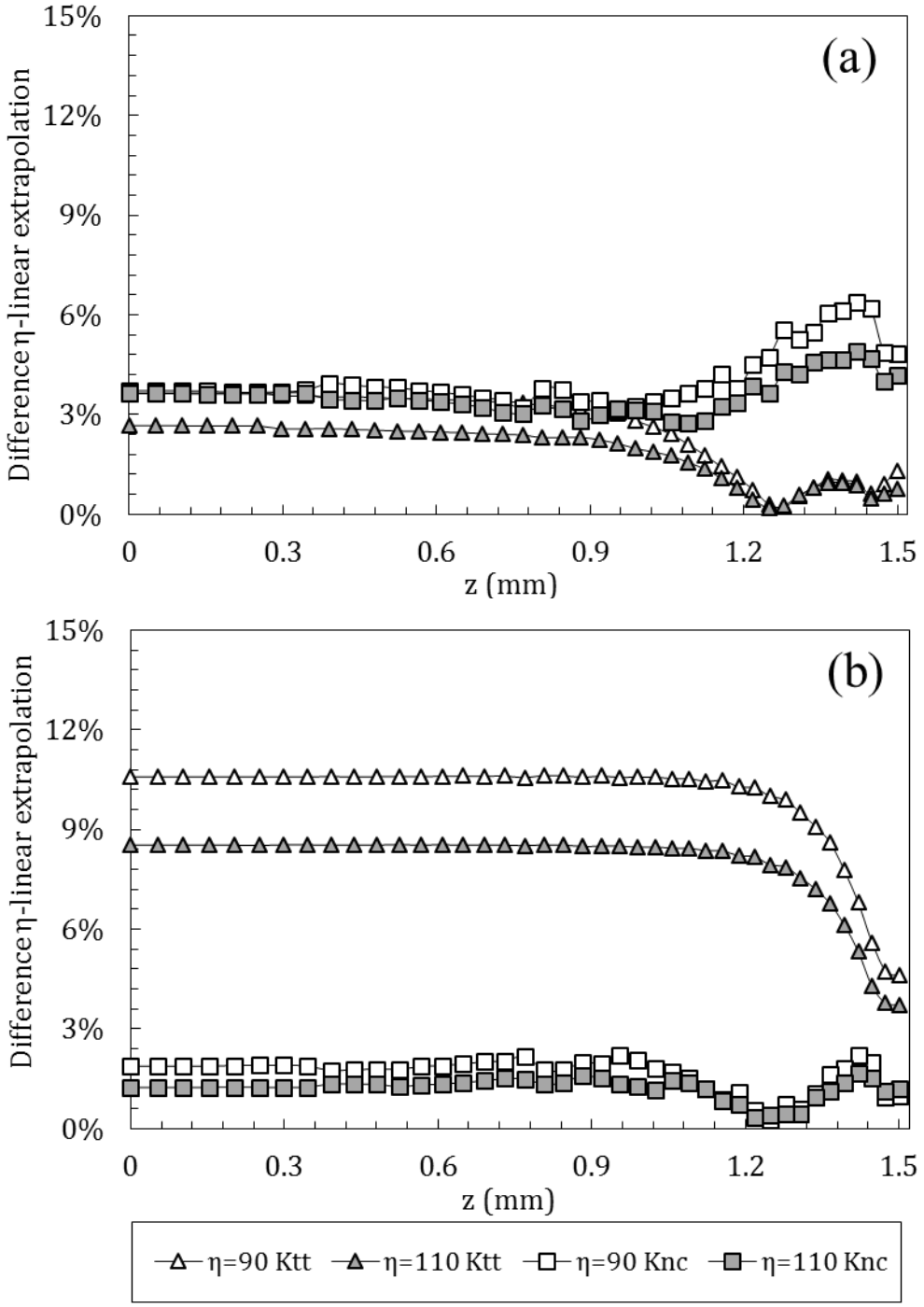

Figure 11. Devation of opening (a) and closure (b) results considering linear extrapolation and η for both criteria. K_{max}=25MPa·m$^{1/2}$ and R=0.1.

Continuing with the analysis of crack closure values, results for R=0.1 are shown in Fig. 12. In this case, it is important to note two different issues. On one hand, the difference between the tip tension values obtained considering an ideal element size or η=90, is in the order of 5% at the surface and 10% in the mid-plane. The source of this difference is like before. There is a great dependence of stress values at the

crack tip with the minimum element size. This yields linear behaviour of the tip tension results with the element size.

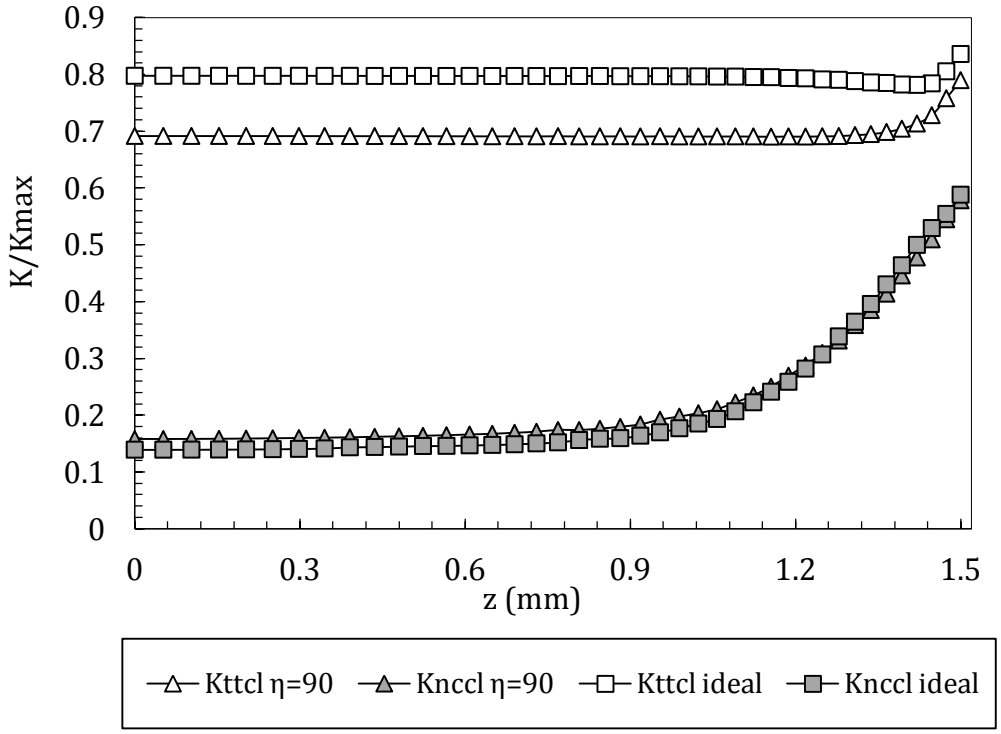

Figure 12. Closure results considering ideal element size or η=90. K_{max}=25MPa·m$^{1/2}$ and R=0.1

3.3. Mesh refinement along the thickness

In three-dimensional modelling, to analyse the influence of the element size along the thickness is necessary apart from analysing the minimum element size in the direction of the crack growth.

In the firsts three-dimensional analyses found in the literature, the number of through-the-thickness elements were very limited by the computational cost. In this way, Chermahini et al. [18] considered 4 elements, Carlyle and Dodds [47] 5 elements and Alizadeh et al. [31] 10 elements. The first numerical analysis which employs a large number of through-the-thickness elements was published by Gonzalez-Herrera [30] who considered 100, 50 and 35 elements in 12, 6 and 3mm specimen thicknesses, respectively. The number of through-the-thickness elements was determined based in a maximum shape ratio near the crack front and equal to 6. No specific evaluation of the error incurred due to this parameter was performed. Later fracture mechanic numerical studies based on the same specimen geometry proved that this fine mesh along the thickness was an important issue to consider in order to capture properly the abrupt transitory behaviour close to the surface [24,48,49].

In this section, the influence of the number of through-the-thickness elements on the results in terms of opening and closure values is analysed. As in the previous section, a 3mm specimen thickness under a load which corresponds to a stress intensity factor K=25MPa·m$^{1/2}$, R=0.3 and η=90 is considered. Four different number of through-the-thickness elements have been considered, ranging from 10 to 60 elements.

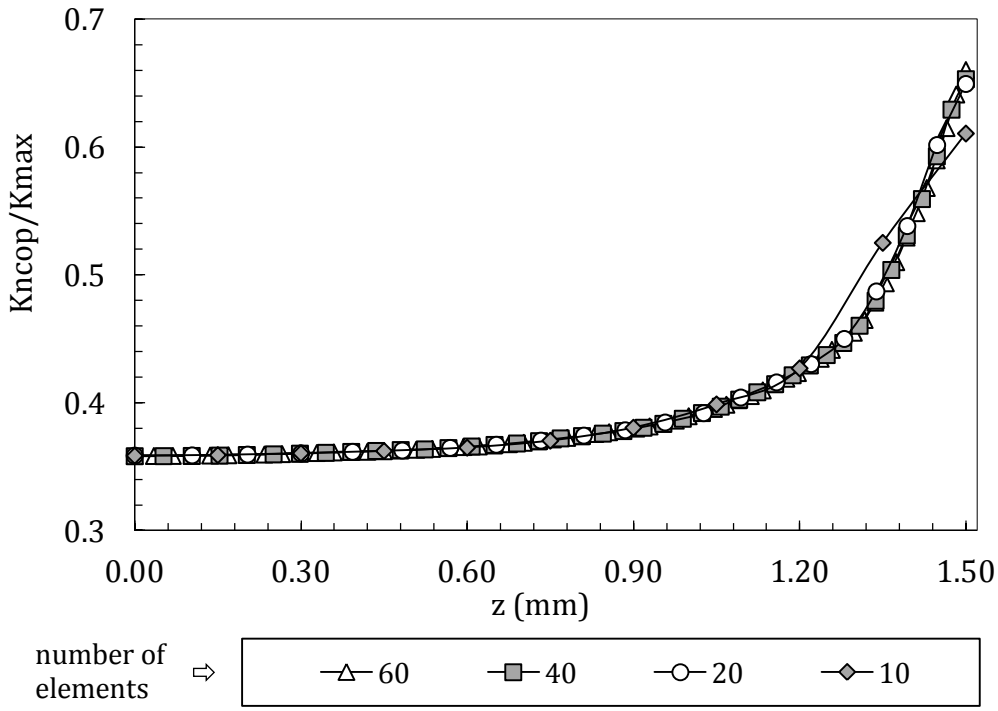

Figure 13. Influence of the number of through-the-thickness elements on node contact crack opening values, K_{max}=25MPa·m$^{1/2}$, R=0.3 and η=90.

Fig. 13 shows the evolution of the opening and closure values along the thickness with the number of through-the-thickness elements. Only the node contact opening criterion values are presented. The behaviour of the rest of them are similar and not provide meaningful information.

This figure shows that the results collapse for a number of through-the-thickness elements equal or greater than 20 elements. Comparing the results corresponding to 20 and 60 elements, the greatest difference occurs at the element on the surface for the tip tension criterion being the difference of the order of 4%. The difference between the rest of elements along the thickness, and for both criteria, can be considered as negligible.

Same conclusion is obtained when considering the transition zone. Fig.14 shows the evolution of the transition zone values for the different considered criteria. It can be seen that results are pretty stable with the number of through-the-thickness elements when they are higher than 20 elements.

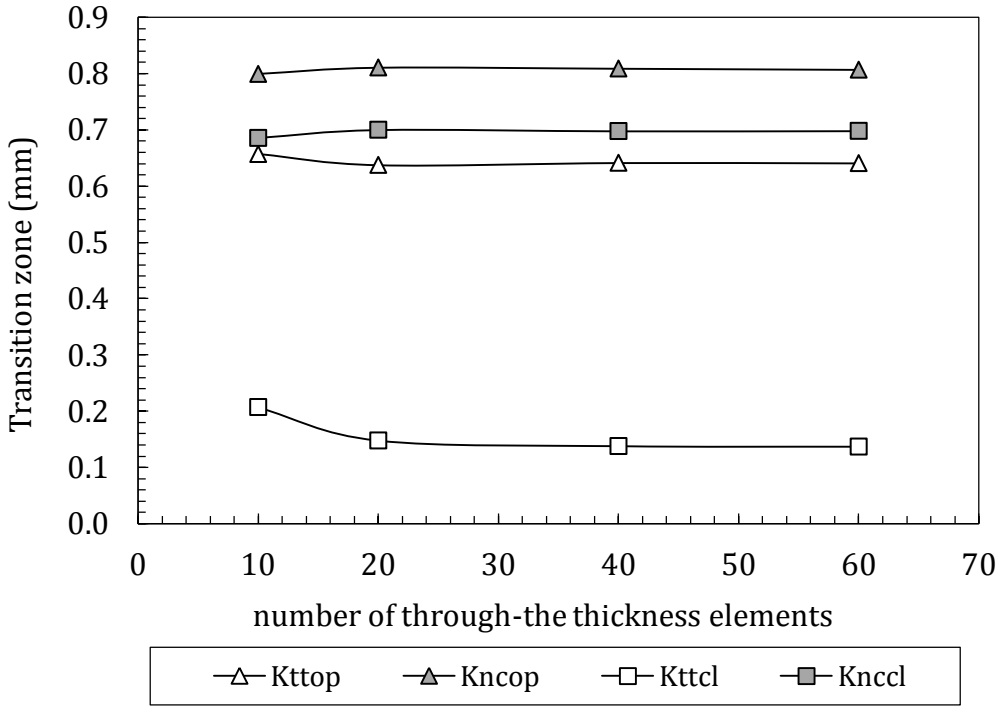

Figure 14. Influence of the number of through-the-thickness elements on the transition zone values. K_{max}=25MPa·m$^{1/2}$, R=0.3 and η=90.

4. DISCUSSION

Time consumption is a key parameter in this kind of analysis and has to be taken into consideration. Thus, while a R=0.3 and η=90 case takes about 50 hours to complete the solution, a R=0.3 and η=110 takes about 132 hours. An i7 processor with 8Gb RAM has been used for this analyses.

Coming back to Fig. 12, the difference between the results obtained with both criteria is remarkable as previous studies have stated [15,43]. When crack opening was analysed in Fig. 10, the conclusion was drawn that both criteria tend to the same results. However, it can be observed that the same does not occur with closure, the results being actually different. This apparently anomalous behaviour agrees with previous results obtained in bi-dimensional analysis in which the plane stress state was considered. Even for some others focused on the plane strain state, the node contact criterion was neglected because some randomness appeared in the results [15,50]. This was analysed by McClung et al. [51] and was justified because the length of the plastic wake was much smaller than in plane stress. Other authors like de Matos

and Nowell [52] just came to the conclusion that to calculate the closing stresses, the tip tension criterion was not appropriate. In that study, the crack tip was compressive during the whole unloading cycle. A more recent study [53] determined that bi-dimensional numerical models employed in plane strain analysis are not optimised due to the small number of loading cycles between increments, a crack propagation that is too short, and oversized finite elements.

From this analysis, the conclusion can be drawn that the crack closure results obtained by the node contact criterion are simply different from the ones obtained by the tip tension criterion. The node contact results are numerically stable, almost constant, with the element size. In the bi-dimensional analysis, as the scale reference is Dugdale's plastic zone size, which in plane strain is much smaller than in plane stress, the number of elements necessary to obtain the convergence is higher. But in the 3D analysis, the convergence is reached with bigger element sizes. In this case, the 3D model gives stability to the results.

There are many different opinions about the coincidence or not of opening and closure values. The numerical results reported in some papers, in some cases are nearly equivalent, in others the opening stresses are higher than the closure ones [11,50,54], while in others, the trend is just the opposite [18,40,37,45].

As can be seen in Fig. 7, which shows the opening and closure values along the thickness for R=0.1 and 0.3 respectively, there is a huge dependence on the plane state and the closure criterion considered for this particular case. At the surface (plane stress conditions), the closure and opening values for both criteria are really close, while in the mid-plane, there is a significant difference. On the other hand, the closure results are higher than the opening ones when the tip tension criterion is employed, while the opposite occurs when the node contact criterion is used.

This conclusion based on displacements is consequent with the analysis of CTOD [55]. If the vertical displacements of the first node behind the crack tip is analysed and the crack is initially closed, the load increase opens the crack elastically. There is plastic deformation if the load keeps increasing. The plastic deformation of the crack tip during loading is responsible for a lower value of crack closure compared with crack opening.

Finally, the R=0.7 cases have been analysed. It has been observed that there is no closure and the crack is always open all along the thickness when considering the node contact criteria. Just a little part near the surface is closed before reaching the K_{min}, when considering the tip tension criteria.

5. CONCLUSIONS

The influence of the minimum element size on crack opening and closure results has been analysed considering a three-dimensional model. Two different criteria have been considered to determine the opening or closure state, one based on the stress at the crack front (tip tension) and other one based on the contact status of the first node behind the crack front (node contact). It has been shown that the results depend on the minimum element size near the crack front.

A linear relationship between the opening and closure values and the minimum element size has been identified. This behaviour is similar to those observed in the bi-dimensional case.

Following the strategy suggested for bi-dimensional problems, an objective value corresponding to an ideal zero mesh size can be calculated by means of a linear extrapolation of three different results from models with different minimum element size.

With this objective value, the error committed with the different mesh sizes has been evaluated. In terms of this error, mesh recommendation for the different criterion can be summarised as follows:

- Regarding the tip tension criterion, the recommended minimum element size would be $\delta<0.015$, which implies a minimum element size at the crack tip in the order of 60 divisions of Dugdale's plastic zone size.

- Considering the node contact criterion, the requirement is lower and the minimum element size would be $\delta<0.03$, which implies a minimum element size at the crack tip in the order of 33 divisions of Dugdale's plastic zone size

- The number of through the thickness elements has been analysed. The size of the element at the surface has been considered half the size of the element next to the mid plane of the specimen. Twenty elements are recommended for both criteria and for a specimen thickness of 3mm modelled with symmetry.

Finally, it must be remarked that while the opening values calculated with the different criterion follows the same trend, closure values are completely different. This is also in agreement with bi-dimensional observation and is related with the asymmetry of the load cycle. These differences are higher at the interior than at the surface of the specimen.

Acnkowledgment

This work has been supported by the Ministerio de Economía y Competitividad of the Spanish Government through grant reference MAT2016-76951-C2-2-P.

References

[1] Ritchie RO, Suresh S, Moss CM. Near-Threshold Fatigue Crack Growth in 2 1/4 Cr-1Mo Pressure Vessel Steel in Air and Hydrogen. J Eng Mater Technol 1980;102:293–9.

[2] Suresh S, Ritchie RO. On the influence of fatigue underloads on cyclic crack growth at low stress intensities. Mater Sci Eng 1981;51:61–9. doi:10.1016/0025-5416(81)90107-5.

[3] Suresh S, Ritchie RO. A geometric model for fatigue crack closure induced by fracture surface roughness. Metall Trans A 1982;13:1627–31. doi:10.1007/BF02644803.

[4] Elber W. Fatigue crack closure under cyclic tension. Eng Fract Mech 1970;2:37–45.

[5] Elber W. The significance of fatigue crack closure. Damage Toler. Aircr. Struct., vol. STP 486, Philadelphia: American Society for Testing and Materials; 1971, p. 230–42.

[6] Cochran KB, Dodds RH, Hjelmstad KD. The role of strain ratcheting and mesh refinement in finite element analyses of plasticity induced crack closure. Int J Fatigue 2011;33:1205–20. doi:10.1016/j.ijfatigue.2011.03.005.

[7] Antunes F V., Camas D, Correia L, Branco R. Finite element meshes for optimal modelling of plasticity induced crack closure. Eng Fract Mech 2015;142:184–200. doi:10.1016/j.engfracmech.2015.06.007.

[8] Antunes F V, Rodrigues DM. Numerical simulation of plasticity induced crack closure: Identification and discussion of parameters. Eng Fract Mech 2008;75:3101–20. doi:10.1016/j.engfracmech.2007.12.009.

[9] Gonzalez-Herrera A, Zapatero J. Numerical study of the effect of plastic wake on plasticity-induced fatigue crack closure. Fatigue Fract Eng Mater Struct 2009;32:249–60. doi:10.1111/j.1460-2695.2009.01335.x.

[10] Newman JC. A Finite-Element analysis of fatigue crack closure. ASTM STP 590, Philadelphia,

PA: 1976, p. 281–301.

[11] McClung RC, Sehitoglu H. On the finite element analysis of fatigue crack closure-1. Basic modeling issues. Eng Fract Mech 1989;33:237–52.

[12] Solanki K, Daniewicz SR, Newman JC. Finite element modeling of plasticity-induced crack closure with emphasis on geometry and mesh refinement effects. Eng Fract Mech 2003;70:1475–89. doi:10.1016/S0013-7944(02)00168-6.

[13] Roychowdhury S, Dodds Jr. RH. A numerical investigation of 3-D small-scale yielding fatigue crack growth. Eng Fract Mech 2003;70:2363–83. doi:10.1016/S0013-7944(03)00003-1.

[14] Antunes F V, Borrego LFP, Costa JD, Ferreira JM. A numerical study of fatigue crack closure induced by plasticity. Fatigue Fract Eng Mater Struct 2004;27:825–35. doi:10.1111/j.1460-2695.2004.00738.x.

[15] González-Herrera A, Zapatero J. Influence of minimum element size to determine crack closure stress by the finite element method. Eng Fract Mech 2005;72:337–55.

[16] S.-J. P, Y.-Y. E, J.-H. S. Determination of the most appropriate mesh size for a 2-D finite element analysis of fatigue crack closure behaviour. Fatigue Fract Eng Mater Struct 2007;20:533–45. doi:10.1111/j.1460-2695.1997.tb00285.x.

[17] Jiang Y, Feng M, Ding F. A reexamination of plasticity-induced crack closure in fatigue crack propagation. Int J Plast 2005;21:1720–40. doi:http://dx.doi.org/10.1016/j.ijplas.2004.11.005.

[18] Chermahini RG. Three-dimensional elastic-plastic finite-element analysis of fatigue crack growth and closure. Old Dominion University, 1986.

[19] Chermahini RG, Shivakumar KN, Newman JC. Three-dimensional finite-element simulation of fatigue crack growth and closure. ASTM STP 982, Philadelphia, PA: 1988, p. 398–413.

[20] Chermahini RG, Shivakumar KN, Newman Jr JC, Blom AF. Three-Dimensional aspects of plasticity-induced fatigue crack closure. Eng Fract Mech 1989;34:393–401. doi:DOI: 10.1016/0013-7944(89)90152-5.

[21] Chermahini RG, Blom AF. Variation of crack-opening stresses in three-dimensions: finite thickness plate. Theor Appl Fract Mech 1991;15:267–76. doi:10.1016/0167-8442(91)90025-F.

[22] Chermahini RG, Palmberg B, Blom AF. Fatigue crack growth and closure behaviour of semicircular and semi-elliptical surface flaws. Int J Fatigue 1993;15:259–63. doi:10.1016/0142-1123(93)90374-Y.

[23] Newman JC, Bigelow CA, Shivakumar KN. Three-dimensional elastic-plastic finite-element analyses of constraint variations in cracked bodies. Eng Fract Mech 1993;46:1–13. doi:10.1016/0013-7944(93)90299-8.

[24] Camas D, Garcia-Manrique J, Gonzalez-Herrera A. Crack front curvature: Influence and effects on the crack tip fields in bi-dimensional specimens. Int J Fatigue 2012;44:41–50.

[25] Branco R, Rodrigues DM, Antunes F V. Influence of through-thickness crack shape on plasticity induced crack closure. Fatigue Fract Eng Mater Struct 2008;31:209–20.

[26] Branco R, Antunes FV, Martins RF. Modelling fatigue crack propagation in CT specimens. Fatigue Fract Eng Mater Struct 2008;31:452–65. doi:10.1111/j.1460-2695.2008.01241.x.

[27] Gardin C, Fiordalisi S, Sarrazin-Baudoux C, Gueguen M, Petit J. Numerical prediction of crack front shape during fatigue propagation considering plasticity-induced crack closure. Int J Fatigue 2016;88:68–77. doi:10.1016/J.IJFATIGUE.2016.03.018.

[28] Branco R, Antunes FV, Costa JD. A review on 3D-FE adaptive remeshing techniques for crack growth modelling. Eng Fract Mech 2015;141:170–95. doi:10.1016/J.ENGFRACMECH.2015.05.023.

[29] Antunes FV, Sousa T, Branco R, Correia L. Effect of crack closure on non-linear crack tip parameters. Int J Fatigue 2015;71:53–63. doi:10.1016/J.IJFATIGUE.2014.10.001.

[30] Gonzalez-Herrera A, Zapatero J. Tri-dimensional numerical modelling of plasticity induced fatigue crack closure. Eng Fract Mech 2008;75:4513–28. doi:10.1016/j.engfracmech.2008.04.024.

[31] Alizadeh H, Hills DA, de Matos PFP, Nowell D, Pavier MJ, Paynter RJ, et al. A comparison of two and three-dimensional analyses of fatigue crack closure. Int J Fatigue 2007;29:222–31. doi:10.1016/j.ijfatigue.2006.03.014.

[32] Vor K, Gardin C, Sarrazin-Baudoux C, Petit J. Wake length and loading history effects on crack closure of through-thickness long and short cracks in 304L: Part II - 3D numerical simulation.

Eng Fract Mech 2013;99. doi:10.1016/j.engfracmech.2013.01.014.

[33] Camas D, Garcia-Manrique J, Gonzalez-Herrera A. Numerical study of the thickness transition in bi-dimensional specimen cracks. Int J Fatigue 2011;33:921–8.

[34] Camas D, Lopez-Crespo P, Gonzalez-Herrera A, Moreno B. Numerical and experimental study of the plastic zone in cracked specimens. Eng Fract Mech 2017;185:20–32. doi:10.1016/j.engfracmech.2017.02.016.

[35] Zhang XP, Ye L, Mai YW, Wang CH. Characterization of the opening/closure behaviour of short fatigue cracks under cyclic loading and its influence on crack growth. In: Dyskin AV, Hu X, E. S, editors. Struct. Integr. Fract., 2002, p. 213–7.

[36] Zapatero J, Gonzalez-Herrera A. Advances in the numerical modelling of fatigue crack closure using finite elements. In: Lignelli AF, editor. Fatigue crack growth Mech. Behav. Predict., New York: Nova Science Publishers; 2009, p. 83–124.

[37] Wu J, Ellyin F. A study of fatigue crack closure by elastic-plastic finite element analysis for constant-amplitude loading. Int J Fract 1996;82:43–65.

[38] Fleck NA. Finite element analysis of plasticity-induced crack closure under plane strain conditions. Eng Fract Mech 1986;25:441–9.

[39] Solanki K, Daniewicz SR, Newman JC. A new methodology for computing crack opening values from finite element analyses. Eng Fract Mech 2004;71:1165–75. doi:10.1016/S0013-7944(03)00113-9.

[40] Wei L-W, James MN. A study of fatigue crack closure in polycarbonate CT specimens. Eng Fract Mech 2000;66:223–42. doi:DOI: 10.1016/S0013-7944(00)00014-X.

[41] Zapatero J, Moreno B, González-Herrera A. Fatigue crack closure determination by means of finite element analysis. Eng Fract Mech 2008;75:41–57. doi:10.1016/j.engfracmech.2007.02.020.

[42] Roychowdhury S, Dodds RH. Three-dimensional effects on fatigue crack closure in small-scale yielding regime - a finite element study. Fatigue Fract Eng Mater Struct 2003;26:663–73.

[43] de Matos PFP, Nowell D. Numerical simulation of plasticity-induced fatigue crack closure with emphasis on the crack growth scheme: 2D and 3D analyses. Eng Fract Mech 2008;75:2087–114. doi:10.1016/j.engfracmech.2007.10.017.

[44] Murakami Y. Stress Intensity Factors Handbook. United States: Pergamon Books; 1987.

[45] Newman JC. A finite-element analysis of fatigue crack closure. NASA Tech Memo X-72005 1974.

[46] ANSYS. User's manual, v.13. 2009.

[47] Carlyle AG, Dodds RH. Three-dimensional effects on fatigue crack closure under fully-reversed loading. vol. 74. 2007. doi:10.1016/j.engfracmech.2006.06.002.

[48] Garcia-Manrique J, Camas D, Gonzalez-Herrera A. Study of the stress intensity factor analysis through thickness: methodological aspects. Fatigue Fract Eng Mater Struct 2017;40. doi:10.1111/ffe.12574.

[49] Garcia-Manrique J, Camas-Peña D, Lopez-Martinez J, Gonzalez-Herrera A. Analysis of the stress intensity factor along the thickness: The concept of pivot node on straight crack fronts. Fatigue Fract Eng Mater Struct 2018;41:869–80. doi:10.1111/ffe.12734.

[50] Fleck NA, Newman JC. Analysis of crack closure under plane strain conditions. ASTM STP 982, Philadelphia, PA: 1988, p. 319–41.

[51] McClung RC, Thacker BH, Roy S. Finite element visualization of fatigue crack closure in plane stress and plane strain. Int J Fract 1991;50:27–49.

[52] de Matos PFP, Nowell D. On the accurate assessment of crack opening and closing stresses in plasticity-induced fatigue crack closure problems. Eng Fract Mech 2007;74:1579–601. doi:10.1016/j.engfracmech.2006.09.007.

[53] Antunes FV, Chegini AG, Branco R, Camas D. A numerical study of plasticity induced crack closure under plane strain conditions. Int J Fatigue 2015;71:75–86. doi:10.1016/j.ijfatigue.2014.03.016.

[54] McClung RC, Sehitoglu H. On the finite element analysis of fatigue crack closure—2. Numerical results. Eng Fract Mech 1989;33:253–72. doi:DOI: 10.1016/0013-7944(89)90028-3.

[55] Antunes FV, Rodrigues SM, Branco R, Camas D. A numerical analysis of CTOD in constant amplitude fatigue crack growth. Theor Appl Fract Mech 2016;85. doi:10.1016/j.tafmec.2016.08.015.

Highlights

- This paper is a three dimensional study of the influence of the element size on the plasticity induced crack closure phenomenon. There are a great number of previous bi-dimensional studies, but, to the best knowledge of the authors, this is the first attempt made considering a three-dimensional model.
- In this study, the crack closure evolution along the specimen thickness as a function of the element size is analysed.
- A methodology to determine the closure/opening values for an ideal mesh size is presented and the differences between these values and the ones obtained considering a given element size are presented.
- The mesh refinement along the thickness is made.
- The transition zones for each considered criterion are determined.
- Classical bi-dimensional recommendations are updated.